SIAM J. NUMER. ANAL.
Vol. 56, No. 3, pp. 1942–1960

ASYMPTOTICALLY COMPATIBLE SCHEMES FOR STOCHASTIC HOMOGENIZATION*

QI SUN†, QIANG DU‡, AND JU MING§

Abstract. In this paper, we study the numerical solution of elliptic homogenization problems with stationary and ergodic coefficients characterized by a small length scale ε. The issue of asymptotic compatibility as $\varepsilon \to 0$ is examined for a number of different numerical approximations, which enables us to construct robust discretization schemes to eliminate the resonance and underresolution errors caused by the inappropriate use of base functions. In addition to the study of effective characteristics based on particular sample realizations that are subject to random effects, we also consider approximations by numerically evaluating the expectation of realized values. When the Monte Carlo finite element method is applied for the latter, error estimation is derived to guide parameter choices so as to further enhance the computational efficiency by performing relatively few samples while attaining high accuracy. Numerical experiments are presented to validate and supplement our theoretical findings.

Key words. stochastic homogenization, asymptotic compatibility, multiscale finite element method, Monte Carlo method

AMS subject classifications. 74Qxx, 35R60, 78M31

DOI. 10.1137/17M1132604

1. Introduction.

Multiscale models have become useful tools in various applications with many of them rife with uncertainties. In many cases, such as heterogeneous materials and porous media, the complicated small-scale details may be averaged out on macroscopic scales, and the characterization of effective property can be highly desirable in practice. In this paper, we consider multiscale elliptic partial differential equations (PDEs) with stationary, ergodic, and uniform coercive coefficients, that is, for a bounded Lipschitz domain D and a given $f \in H^{-1}(D)$, find $u_\varepsilon(x,\omega) : D\times\Omega \to \mathbb{R}$ such that for almost everywhere (a.e.) ω in a set of outcomes Ω,

$$\begin{cases} -\nabla \cdot \left(a_\varepsilon^T(x,\omega)\nabla u_\varepsilon(x,\omega)\right) = f(x) & \text{in } D, \\ u_\varepsilon(x,\omega) = 0 & \text{on } \partial D, \end{cases} \tag{1}$$

where $a_\varepsilon^T(x,\omega)$ is a random coefficient parametrized by $0 < \varepsilon \ll 1$ that, for example, describes the permeability or conductivity field that involves uncertainty [31], and T represents a measure preserving dynamical system which will be specified later. It is well known that the weak solution to (1) admits homogenization almost surely and the effective (or homogenized) solution could be found by solving certain auxiliary

*Received by the editors May 31, 2017; accepted for publication (in revised form) April 25, 2018; published electronically June 28, 2018.

http://www.siam.org/journals/sinum/56-3/M113260.html

Funding: This work was funded in part by NSFC-91630207 and NSFC-U1530401, the China Scholarship Council, NSF DMS-1558744, NSF DMS-1719699, AFOSR MURI Center for Material Failure Prediction Through Peridynamics, and ARO MURI grant W911NF-15-1-0562.

†Division of Applied and Computational Mathematics, Beijing Computational Science Research Center, Beijing 100193, China, and School of Mathematical Science, University of Science and Technology of China, Hefei 230026, China (sunqi@csrc.ac.cn, sunqi@mail.ustc.edu.cn).

‡Applied Physics and Applied Mathematics and Data Science Institute, Columbia University, New York, NY 10027 (qd2125@columbia.edu).

§School of Mathematics and Statistics, Huazhong University of Science and Technology, Wuhan 430000, China (jming@hust.edu.cn).

problems [25, 26, 30]. Additional studies on the effects of random fluctuation and numerical approximations can be found, e.g., in [1, 2, 5, 7, 9, 10, 17, 24, 25] and the references cited therein. Indeed, while the effective coefficient in the one-dimensional case can be determined explicitly, no closed-form expressions are available for generic high-dimensional problems due to the abstract statements of auxiliary problems [10]. Hence, numerical realizations of stochastic homogenization are often the only viable approach for approximating the effective solution. In recent years, numerical methods for PDEs with random data and input have been studied extensively; we refer to [23] for a recent survey.

An issue that naturally arises in the practical implementation of the numerical stochastic homogenization is to investigate how the discretization scale should correspond to the modeling parameter to achieve numerical convergence. Similar issues are often encountered in many other applications that involve parametrized problems characterized by some physical scaling parameters, such as periodic homogenization problems with a small period [24] and high-contrast problems with additional small scales in the heterogeneous field [14]. We also refer to [15, 34] for more discussions and additional references on numerical solutions of parameterized problems, in which the discretization of nonlocal problems involving a horizon parameter describing the scale of nonlocal interactions is studied.

A major contribution of this work is to introduce the notion of asymptotically compatible schemes developed in [34] for numerical stochastic homogenization. Such schemes offer robust discretizations that converge uniformly to the homogenized solution u_0. Specifically, let h be the discretization scale, and $u_\varepsilon^h(x,\omega)$ denotes the pathwise numerical solution to (1). Analogous to the diagram given in [34], we want to check whether the diagram in Figure 1 commutes.

Note that the convergent paths (i)–(iv) are presented by fixing one of the parameters h and ε while sending the other one to zero, and the three other different regimes (v)–(vii) are introduced as both h and ε tend to zero simultaneously. For standard finite element methods (FEMs), whose spaces are asymptotically dense in the solution space, we prove that the diagram commutes except for the path (ii) due to the under-resolution. To correctly pass to the limit in path (ii), many upscaling methods, e.g., multiscale finite element methods (MsFEMs) [24] and heterogeneous multiscale methods (HMMs) [2], are developed to find accurate approximations of

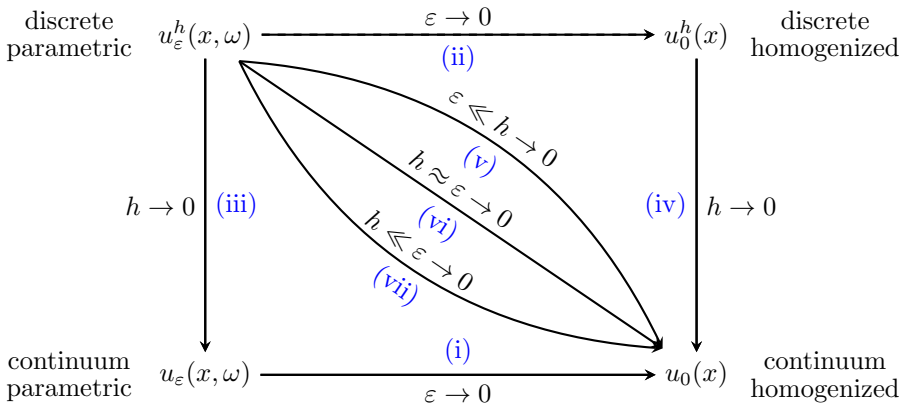

FIG. 1. *A diagram describing the convergence results of numerical homogenization.*

the homogenized solution without fully resolving the microscopic features. These approaches can enhance the convergence along most paths shown in the diagram, but a straightforward implementation of MsFEMs suffers from resonance between the modeling parameter and the discretization scale, that is, it might not correctly pass to the limit for path (vi) [24]. Intuitively, the reason for not getting the correct convergence in the latter case is that the MsFEM space may not be asymptotically dense in solution space. As a result, one could construct extended MsFEMs (X-MsFEMs) by certain enrichments of the approximation space such that the diagram in Figure 1 fully commutes. Systematic discussions of the above account are given in this work.

Additionally, the random fluctuation theory for stochastic homogenization shows that the convergent paths (i)–(iv) in Figure 1 are in the sense of distribution [7]. The numerical evaluation of the effective solution could be extremely slow due to the influence of random input data. The corresponding expected value, which also converges to the effective solution, may provide a more attractive alternative where the convergence is less susceptible to the effects of random fluctuations. To evaluate the expectation, we consider the Monte Carlo (MC) finite element approach

$$\mathcal{Q}^{\mathrm{MC}} = \frac{1}{n}\sum_{i=1}^{n} u_\varepsilon^h(x,\omega_i), \tag{2}$$

where $\{u_\varepsilon^h(x,\omega_i) \in H_0^1(D)\}_{i=1}^n$ solves problem (1) numerically with independent and identically distributed random input data $\{a_\varepsilon^T(x,\omega_i)\}_{i=1}^n$. By mimicking a similar diagram in Figure 1, the numerical scheme (2) is shown to inherit the property of asymptotic compatibility from the numerical sample realizations. It is well known that the MC methods are useful tools to break the curse of dimensionality and may incur enormous computational cost since the sample size required is typically large and does not change with respect to (w.r.t.) the modeling parameter [1]. However, for stochastic homogenization problems with deterministic effective characteristics, a key observation is that both the numerical sample realization and its expected value can converge to the same effective solution. This enables us to perform relatively few simulations to attain high accuracy, in contrast to the conventional half order convergence of the MC methods. Moreover, specific error estimation is derived in this paper for the determination of the optimal sample size.

Our paper is organized as follows. In section 2, some preliminary description of stochastic homogenization is introduced. Then in section 3, after a brief review of homogenization results for multiscale elliptic PDEs with stationary and ergodic coefficients in the continuous sense, the asymptotic compatibilities of numerical sample realizations using FEMs, MsFEMs, and X-MsFEMs are studied. Next, in section 4, we first prove that the numerical expectation can converge to the same effective solution while its MC FE approach inherits the property of asymptotic compatibility for all $n \in \mathbb{Z}_+$, then detailed error estimates are derived to further enhance the numerical efficiency. Finally, some concluding remarks are given in section 5.

2. Preliminaries. We first introduce the function spaces and notation used in this paper and some basic knowledge of ergodic theory and compensated compactness.

2.1. Stochastic function spaces and notation. Throughout this paper, we adopt the notation in [18] for the classical Sobolev spaces. To be specific, let d be a positive integer and D be an open, connected, bounded, and convex subset of $\mathbb{R}^d$ with polygonal boundary ∂D. $H^r(D)$, $r \in \mathbb{Z}_+$, is a Sobolev space equipped with the inner product $(\cdot,\cdot)_{H^r(D)}$ and the induced norm $\|\cdot\|_{H^r(D)}$. Clearly, $\|\cdot\|_{H^r(D)}$ is equivalent to

the seminorm $|\cdot|_{H^r(D)}$ in $H_0^r(D)$, where $H_0^r(D) := \{v \in H^r(D) : v = 0 \text{ on } \partial D\}$. We use C to denote a generic constant whose value may change with context. Moreover, let $(\Omega, \mathcal{F}, \mu)$ denote a σ-finite probability space, where Ω is a set of outcomes, $\mathcal{F}$ is a σ-algebra of events, and $\mu : \mathcal{F} \to [0,1]$ is a probability measure.

$$\mathbb{E}[X] = \int_\Omega X(\omega)\, d\mu(\omega) \quad \text{and} \quad \mathbb{V}[X] = \mathbb{E}\left[(X - \mathbb{E}[X])^2\right]$$

are the expected value and the variance of the random variable $X(\omega)$.

Let $\mathcal{B}(D)$ be the Borel σ-algebra generated by the open subsets of D; we define the stochastic Sobolev spaces $\mathcal{H}^r(D) = L^2(\Omega; H^r(D))$ consisting of those functions that are assumed to be strongly measurable w.r.t. the product σ-algebra $\mathcal{B}(D) \otimes \mathcal{F}$, whose associated inner product is given as

$$[u, v]_{L^2(\Omega; H^r(D))} = \mathbb{E}\big[(u, v)_{H^r(D)}\big] = \int_\Omega (u, v)_{H^r(D)}\, d\mu,$$

and thus the norm

$$\|v\|^2_{L^2(\Omega; H^r(D))} = \mathbb{E}\big[\|v\|^2_{H^r(D)}\big] = \int_\Omega \|v\|^2_{H^r(D)}\, d\mu.$$

Note that the stochastic Sobolev space $\mathcal{H}^r(D)$ is a Hilbert space and is isomorphic to the tensor product Hilbert space $H^r(D) \otimes L^2(\Omega)$ [6]. For simplicity, let $(\cdot, \cdot) := (\cdot, \cdot)_{L^2(D)}$ and

$$\mathcal{L}^2(D) := L^2(\Omega; L^2(D)) \text{ with norm } \|v\|^2_{\mathcal{L}^2(D)} = \mathbb{E}\left[\|v\|^2_{L^2(D)}\right],$$
$$\mathcal{L}_\infty(D) := L^2(\Omega; L_\infty(D)) \text{ with norm } \|v\|_{\mathcal{L}_\infty(D)} = \mathbb{E}\left[\|v\|_{L_\infty(D)}\right].$$

2.2. Ergodic theory and compensated compactness. We briefly recall the Birkhoff ergodic theorem, Weyl decomposition theorem, and Div-Curl theorem, which are used in proving stochastic homogenization in this paper.

DEFINITION 2.1. *A d-dimensional measure preserving dynamical system is a family of measurable mappings $T_x : \Omega \to \Omega$, parametrized by $x \in \mathbb{R}^d$, satisfying that*

1. *$T_0 = I$ is the identity mapping on Ω;*
2. *$T_x \circ T_y = T_{x+y}$ for all $x, y \in \mathbb{R}^d$;*
3. *the dynamical system is measure preserving in the sense that for every $x \in \mathbb{R}^d$ and every μ-measurable set $\mathcal{E} \in \mathcal{F}$ we have $\mu(T_x^{-1}(\mathcal{E})) = \mu(\mathcal{E})$;*
4. *for any measurable function $f(\omega)$ on Ω, the composition $f(T_x(\omega))$ defined on the Cartesian product $\Omega \times \mathbb{R}^d$ is also measurable.*

Furthermore, the following two statements are equivalent:

5. *the measure preserving dynamical system $T = \{T_x\}_{x \in \mathbb{R}^d}$ is ergodic;*
6. *whenever $f(\omega) \in L^2(\Omega)$ and $f(T_x(\omega)) = f(\omega)$ for all $(\omega, x) \in \Omega \times \mathbb{R}^d$ then f is constant a.e.*

By defining the following notion of mean value for functions defined in $\mathbb{R}^d$, we are able to illustate the Birkhoff ergodic theorem [3, 25].

DEFINITION 2.2. *Let $g(x) \in L^p_{\text{loc}}(\mathbb{R}^d)$ for some $p \geq 1$; a number M_g is called the* mean value *of g if for any Lebesgue measurable bounded set $K \subset \mathbb{R}^d$ with measure $|K| \neq 0$,*

$$g(\varepsilon^{-1}x) \overset{w}{\rightharpoonup} M_g = \lim_{\varepsilon \to 0} \frac{1}{|K|} \int_K g(\varepsilon^{-1}x)\, dx \quad \text{in } L^p_{\text{loc}}(\mathbb{R}^d), \text{ as } \varepsilon \to 0. \tag{3}$$

THEOREM 2.3. *Let $T = \{T_x\}_{x\in\mathbb{R}^d}$ be a measure preserving dynamical system and $f \in L^p(\Omega)$ with $p \geq 1$; then for a.e. $\omega \in \Omega$ the realization $g^T(x,\omega) = f(T_x(\omega))$ possesses a mean value in the sense of formula (3), that is, by defining $g^T_\varepsilon(x,\omega) = g^T(\varepsilon^{-1}x,\omega)$, one has*

$$g^T_\varepsilon(\cdot,\omega) \overset{w}{\rightharpoonup} M_g(\omega) \ \text{ in } L^p_{\mathrm{loc}}(\mathbb{R}^d), \ \text{as } \varepsilon \to 0.$$

In particular, if the system T is ergodic, then for a.e. $\omega \in \Omega$ the mean value above is a constant and

$$g^T_\varepsilon(\cdot,\omega) \overset{w}{\rightharpoonup} \int_\Omega f(\omega)\, d\mu = \mathbb{E}[f] \ \text{ in } L^p_{\mathrm{loc}}(\mathbb{R}^d), \ \text{as } \varepsilon \to 0.$$

Furthermore, a vector field $\boldsymbol{g} \in \boldsymbol{L}^2(\Omega) := \left(L^2(\Omega)\right)^d$ is called solenoidal (resp., potential) if its realization $\boldsymbol{g}\left(T_x(\omega)\right)$, constructed with a measure preserving dynamical system T, is solenoidal (resp., potential) on $\mathbb{R}^d$ for a.e. $\omega \in \Omega$. We define the spaces of potential and solenoidal vector fields by $\boldsymbol{L}^2_{\mathrm{pot}}(\Omega,T)$ and $\boldsymbol{L}^2_{\mathrm{sol}}(\Omega,T)$, respectively. Then, by defining the space

$$\boldsymbol{V}^2_{\mathrm{pot}}(\Omega,T) = \left\{\boldsymbol{g} \in \boldsymbol{L}^2_{\mathrm{pot}}(\Omega,T) : \ \mathbb{E}[\boldsymbol{g}] = \boldsymbol{0}\right\},$$

the Weyl decomposition theorem is stated as follows [25].

THEOREM 2.4. *If the dynamical system T is ergodic, then the following orthogonal decomposition is valid:*

$$\boldsymbol{L}^2(\Omega) = \boldsymbol{V}^2_{\mathrm{pot}}(\Omega,T) \oplus \boldsymbol{L}^2_{\mathrm{sol}}(\Omega,T).$$

Finally, we state a well-known compensated compactness result, namely, the Div-Curl theorem.

THEOREM 2.5. *Let D be a bounded domain in $\mathbb{R}^d$, and let $\boldsymbol{u}_\varepsilon$ and $\boldsymbol{v}_\varepsilon$ be vector fields in $\boldsymbol{L}^2(D)$ such that*

$$\boldsymbol{u}_\varepsilon \overset{w}{\rightharpoonup} \boldsymbol{u}_0 \ \text{ and } \ \boldsymbol{v}_\varepsilon \overset{w}{\rightharpoonup} \boldsymbol{v}_0 \ \text{ in } \boldsymbol{L}^2(D), \ \text{ as } \varepsilon \to 0.$$

If, in addition, the conditions $\nabla \cdot \boldsymbol{u}_\varepsilon \to f$ in $H^{-1}(D)$ and $\operatorname{curl} \boldsymbol{v}_\varepsilon = 0$ are satisfied, then

$$\boldsymbol{u}_\varepsilon \cdot \boldsymbol{v}_\varepsilon \overset{w^\star}{\rightharpoonup} \boldsymbol{u}_0 \cdot \boldsymbol{v}_0, \ \text{ as } \varepsilon \to 0.$$

3. Asymptotically compatible schemes for realization. In this section, after introducing the homogenization results for multiscale elliptic PDEs with stationary and ergodic coefficients in the continuous sense, we study the asymptotic compatibilities for numerical homogenization procedures using FEMs, MsFEMs, and X-MsFEMs. A one-dimensional benchmark numerical test is presented to validate and supplement our theoretical findings.

3.1. Parametric problems and their approximations. Here and in what follows, let $T = \{T_x\}_{x\in\mathbb{R}^d}$ be a family of measure preserving dynamical system that is ergodic, and let $a(\omega) = (a_{ij}(\omega))_{d\times d}$ be a matrix function that belongs to the following space with positive constants a_- and a_+, namely,

$$\begin{aligned}\mathcal{A} = \{a : \Omega \to \mathbb{R}^{d\times d}_{\mathrm{sym}} : \ & a(\omega) \text{ is measurable w.r.t. } \mathcal{F} \text{ and} \\ & 0 < a_-|\boldsymbol{\xi}|^2 \leq \boldsymbol{\xi}\cdot a(\omega)\boldsymbol{\xi} \leq a_+|\boldsymbol{\xi}|^2 < +\infty \text{ for all } \boldsymbol{\xi} \in \mathbb{R}^d, \text{ for a.e. } \omega \in \Omega\}.\end{aligned}$$

In many applications, such as diffusion through porous media and heterogeneous materials (see, for instance, [31] and references therein), the permeability fields typically vary at a small scale due to the randomly oriented pores, and the steady-state diffusion in such media could be described by an elliptic variational problem, parametrized by $0 < \varepsilon \ll 1$ and with random coefficients, that is,

$$
(4)\quad \begin{cases} \text{given } f \in H^{-1}(D),\ \text{find } u_\varepsilon(\cdot,\omega) \in H_0^1(D) \text{ such that for a.e. } \omega \in \Omega, \\ \qquad a_\varepsilon(u_\varepsilon, v) = (f, v) \ \text{ for all } v \in H_0^1(D), \\ \text{where } a_\varepsilon(u,v) = \displaystyle\int_D a_\varepsilon^T(\cdot,\omega)\nabla u \cdot \nabla v \, dx \text{ for all } u, v \in H_0^1(D) \text{ with} \\ \qquad a_\varepsilon^T(x,\omega) = a^T(\varepsilon^{-1}x, \omega) = a\left(T_{\varepsilon^{-1}x}(\omega)\right). \end{cases}
$$

Here and throughout this paper, "∇" means differentiation w.r.t. the spatial variable $x \in D$ only, and the coefficient $a_\varepsilon^T(x,\omega)$ is stationary and ergodic by its construction.

It is well known that the sequence of coefficients $\{a_\varepsilon^T(x,\omega)\}_{\varepsilon>0}$ G-converges to an effective coefficient $a_0 \in \mathcal{A}$ at a constant value [25], that is, the weak solutions to problem (4) satisfy the following convergence properties:

(a) $u_\varepsilon(\cdot,\omega) \overset{w}{\rightharpoonup} u_0$ in $H_0^1(D)$ for a.e. $\omega \in \Omega$;

(b) $a_\varepsilon^T(\cdot,\omega)\nabla u_\varepsilon(\cdot,\omega) \overset{w}{\rightharpoonup} a_0 \nabla u_0$ in $\boldsymbol{L}^2(D)$ for a.e. $\omega \in \Omega$,

as $\varepsilon \to 0$, where u_0 solves the homogenized problem

$$
(5)\quad \begin{cases} \text{given the same } f \in H^{-1}(D),\ \text{find } u_0(x) \in H_0^1(D) \text{ such that} \\ \qquad a_0(u_0, v) = (f, v) \ \text{ for all } v \in H_0^1(D), \\ \text{where } a_0(u,v) = \displaystyle\int_D a_0 \nabla u \cdot \nabla v \, dx \text{ for } u, v \in H_0^1(D), \text{ and } a_0 \text{ is defined by} \\ \qquad a_0 \boldsymbol{\xi} = \displaystyle\int_\Omega a(\omega)\left(\boldsymbol{\xi} + \boldsymbol{\varphi}_{\boldsymbol{\xi}}(\omega)\right) d\mu \ \text{ for all } \boldsymbol{\xi} \in \mathbb{R}^d, \\ \text{where } \boldsymbol{\varphi}_{\boldsymbol{\xi}}(\omega) \text{ solves the auxiliary problem: find } \boldsymbol{\varphi} \in \boldsymbol{V}_{\text{pot}}^2(\Omega, T) \text{ such that} \\ \qquad \displaystyle\int_D a(\omega)\left(\boldsymbol{\xi} + \boldsymbol{\varphi}(\omega)\right) \cdot \boldsymbol{\vartheta}(\omega) \, d\mu = 0 \ \text{ for all } \boldsymbol{\vartheta} \in \boldsymbol{V}_{\text{pot}}^2(\Omega, T). \end{cases}
$$

Note that for any vector $\boldsymbol{\xi} \in \mathbb{R}^d$, the auxiliary problem in (5) is well-posed and has a unique solution $\boldsymbol{\varphi}_{\boldsymbol{\xi}} \in \boldsymbol{V}_{\text{pot}}^2(\Omega, T)$ which is a linear function of $\boldsymbol{\xi}$ [25].

Although the effective coefficient is explicitly characterized by $a_0 = \left(\mathbb{E}[a^{-1}(\omega)]\right)^{-1}$ in the one-dimensional case [3], no closed-form expressions are available for the general d-dimensional problems. As a result, much attention has been paid in the literature to numerically solving the auxiliary problem to obtain the effective coefficient, e.g., [10, 17] and references therein. Alternatively, the effective properties can also be characterized by solving the problem (4) for a sufficiently small modeling parameter [7].

We consider here the effective solution that is approached by numerically solving the problem (4) with parameter ε chosen small enough, that is,

$$
(6)\quad \begin{cases} \text{given the same } f \in H^{-1}(D),\ \text{find } u_\varepsilon^h(\cdot,\omega) \in V_h \text{ such that for a.e. } \omega \in \Omega, \\ \qquad a_\varepsilon(u_\varepsilon^h, v_h) = (f, v_h) \ \text{ for all } v_h \in V_h, \end{cases}
$$

where V_h is the approximation space, and $u_0^h \in V_h$ can be defined in a similar way.

As such, the question on asymptotic compatibility arises naturally: how about the asymptotic behaviors of the solution to problem (6) as $h \to 0$, $\varepsilon \to 0$, or both? In other words, we want to check whether the diagram in Figure 1 commutes.

3.2. Asymptotic compatibility. Note that the convergent path (i) in Figure 1 is implied by the theory of G-convergence presented in section 3.1. Next, we consider the convergence of Galerkin approximations as $h \to 0$ for a fixed $\varepsilon \in [0, \infty)$, i.e., the paths (iii)–(iv) in Figure 1, which is a conventional numerical analysis question since the ε-scale details are fully resolved [7].

LEMMA 3.1. *For any FEMs whose space V_h is asymptotically dense in the solution space, by the Galerkin approximation, there exists a generic constant $C > 0$ such that*

$$\|u_\varepsilon(\cdot,\omega) - u_\varepsilon^h(\cdot,\omega)\|_{H_0^1(D)} \le C \inf_{v_h \in V_h} \|u_\varepsilon(\cdot,\omega) - v_h\|_{H_0^1(D)} \to 0, \quad \text{as } h \to 0,$$

for arbitrary but fixed $\varepsilon \in [0, \infty)$ and a.e. $\omega \in \Omega$.

Now we consider the situation where both ε and h are sent to zero simultaneously, i.e., the convergent paths (v)–(vii) in Figure 1, and the result is presented in the following theorem, which relies on a notion of asymptotically dense approximation spaces [34]. That is, in the current context, the FEM spaces (that may be constructed with dependence on ε) remain dense in $H_0^1(D)$ as $(\varepsilon, h) \to (0, 0)$.

THEOREM 3.2. *For any conforming FEMs whose space is asymptotically dense in the solution space, the pathwise solution to* (6) *satisfies the convergence properties*

$$u_\varepsilon^h(\cdot,\omega) \overset{w}{\rightharpoonup} u_0 \text{ in } H_0^1(D) \quad \text{and} \quad u_\varepsilon^h(\cdot,\omega) \to u_0 \text{ in } L^2(D), \text{ for a.e. } \omega \in \Omega,$$

for any sequences $\varepsilon \to 0$ and $h \to 0$ simultaneously.

Proof. Step 1. For any sequences $\{\varepsilon_n\}$ and $\{h_n\}$ that tend to 0 as $n \to \infty$, it can be easily deduced from (6) that the sequence of pathwise solutions $\{u_n := u_{\varepsilon_n}^{h_n}(\cdot,\omega)\}$ is uniformly bounded in $H_0^1(D)$ for a.e. $\omega \in \Omega$. Then, by the Banach–Alaoglu theorem, there exist convergent subsequence (not relabeled) and $u_0 := u_0(\cdot,\omega) \in H_0^1(D)$ such that for a.e. $\omega \in \Omega$,

$$u_n \overset{w}{\rightharpoonup} u_0 \ \text{ in } H_0^1(D).$$

Since $H_0^1(D)$ is compactly embedded into $L^2(D)$, we have by the Rellich embedding theorem that, for a.e. $\omega \in \Omega$,

$$u_n \to u_0 \ \text{ in } L^2(D) \ \text{ and } \ \nabla u_n \overset{w}{\rightharpoonup} \nabla u_0 \ \text{ in } \boldsymbol{L}^2(D). \tag{7}$$

Let $a_n := a_{\varepsilon_n}^T(\cdot,\omega)$ and $\boldsymbol{\sigma}_n := a_n \nabla u_n$. Then for a.e. $\omega \in \Omega$, by the boundedness of $\{\boldsymbol{\sigma_n}\}$ in $\boldsymbol{L}^2(D)$, there exists a subsequence (not relabeled) and $\boldsymbol{\sigma}_0 := \boldsymbol{\sigma_0}(\cdot,\omega) \in \boldsymbol{L}^2(D)$ such that

$$\boldsymbol{\sigma}_n \overset{w}{\rightharpoonup} \boldsymbol{\sigma}_0 \ \text{ in } \boldsymbol{L}^2(D). \tag{8}$$

Step 2. Let $\boldsymbol{\xi} \in \mathbb{R}^d$ be fixed but arbitrary and $\boldsymbol{\varphi_\xi}(\omega) \in \boldsymbol{V}_{\text{pot}}^2(\Omega, T)$ be the solution to the auxiliary problem given in (5), and let $\boldsymbol{p}(\omega) := \boldsymbol{\xi} + \boldsymbol{\varphi_\xi}(\omega)$. By definition, we obtain

$$\boldsymbol{p}(\omega) \in \boldsymbol{L}_{\text{pot}}^2(\Omega, T) \ \text{ and } \ \mathbb{E}[\boldsymbol{p}] = \boldsymbol{\xi} + \mathbb{E}[\boldsymbol{\varphi_\xi}] = \boldsymbol{\xi}.$$

Moreover, let $\boldsymbol{q}(\omega) := a(\omega)\boldsymbol{p}(\omega)$, by the auxiliary problem and Theorem 2.4, we have

$$\boldsymbol{q}(\omega) \in \boldsymbol{L}_{\text{sol}}^2(\Omega, T) \ \text{ and } \ \mathbb{E}[\boldsymbol{q}] = \int_\Omega a(\omega)\left(\boldsymbol{\xi} + \boldsymbol{\varphi_\xi}(\omega)\right) d\mu := a_0 \boldsymbol{\xi}. \tag{9}$$

We define $\boldsymbol{p}_n^T(x,\omega) := \boldsymbol{p}(T_{\varepsilon_n^{-1}x}(\omega))$ and $\boldsymbol{q}_n^T(x,\omega) := \boldsymbol{q}(T_{\varepsilon_n^{-1}x}(\omega))$, then by Theorem 2.3, it immediately implies, for a.e. $\omega \in \Omega$,

$$\boldsymbol{p}_n^T(\cdot,\omega) \overset{w}{\rightharpoonup} \mathbb{E}[\boldsymbol{p}] = \boldsymbol{\xi} \ \text{ and } \ \boldsymbol{q}_n^T(\cdot,\omega) \overset{w}{\rightharpoonup} \mathbb{E}[\boldsymbol{q}] = a_0\boldsymbol{\xi} \ \text{ in } \boldsymbol{L}^2(D). \tag{10}$$

Step 3. By the symmetry of $a_n = a(T_{\varepsilon_n^{-1}x}(\omega)) \in \mathcal{A}$, we can write

$$\boldsymbol{\sigma}_n \cdot \boldsymbol{p}_n^T(\cdot,\omega) = (a_n\nabla u_n)\cdot \boldsymbol{p}_n^T(\cdot,\omega) = \nabla u_n \cdot (a_n\, \boldsymbol{p}_n^T(\cdot,\omega)) = \nabla u_n \cdot \boldsymbol{q}_n^T(\cdot,\omega). \tag{11}$$

Note that, on the left-hand side of (11), by (6) and the fact that V_{h_n} is dense in $H_0^1(D)$ as $h_n \to 0$, we have for a.e. $\omega \in \Omega$,

$$\begin{aligned}
\|\nabla\cdot\boldsymbol{\sigma}_n + f\|_{H^{-1}(D)} &= \sup_{\|v\|_{H_0^1(D)}\le 1} |(\nabla\cdot\boldsymbol{\sigma}_n + f, v)| \\
&= \sup_{\|v\|_{H_0^1(D)}\le 1} \left| \int_D \boldsymbol{\sigma}_n \cdot (-\nabla v + \nabla v_{h_n})\, dx + \int_D f(v - v_{h_n})\, dx \right| \\
&\le \sup_{\|v\|_{H_0^1(D)}\le 1} \Big(\|\boldsymbol{\sigma}_n\|_{\boldsymbol{L}^2(D)} \|\nabla v_{h_n} - \nabla v\|_{\boldsymbol{L}^2(D)} \\
&\qquad\qquad + \|f\|_{L^2(D)} \|v - v_{h_n}\|_{L^2(D)} \Big) \\
&\to\ 0, \quad \text{as } n \to \infty,
\end{aligned}$$

that is, $\nabla\cdot\boldsymbol{\sigma}_n \to -f$ in $H^{-1}(D)$. Moreover, by $\boldsymbol{p}_n^T(\cdot,\omega) \in \boldsymbol{L}^2_{\mathrm{pot}}(\Omega,T)$ and $\operatorname{curl}\nabla g = 0$ for any scalar-valued function g, we have $\operatorname{curl}\boldsymbol{p}_n^T(\cdot,\omega) = 0$ for a.e. $\omega \in \Omega$. Then by (8), (10), and Theorem 2.5, we get

$$\boldsymbol{\sigma}_n \cdot \boldsymbol{p}_n^T(\cdot,\omega) \overset{w^\star}{\rightharpoonup} \boldsymbol{\sigma}_0 \cdot \boldsymbol{\xi} \ \text{ for a.e. } \omega \in \Omega. \tag{12}$$

On the other hand, for the right-hand side of (11), we have for a.e. $\omega \in \Omega$, $\nabla\cdot\boldsymbol{q}_n^T(\cdot,\omega) = 0$ by $\boldsymbol{q}_n^T(\cdot,\omega) \in \boldsymbol{L}^2_{\mathrm{sol}}(\Omega,T)$ and $\operatorname{curl}\nabla u_n = 0$. Then by (7), (9), and Theorem 2.5, we have

$$\nabla u_n \cdot \boldsymbol{q}_n^T(\cdot,\omega) \overset{w^\star}{\rightharpoonup} \nabla u_0 \cdot a_0\boldsymbol{\xi} \ \text{ for a.e. } \omega \in \Omega. \tag{13}$$

Since a_n is symmetric and the same can be said about a_0 [25, 33], by the uniqueness of weak limit and (12), (13), we then have for a.e. $\omega \in \Omega$,

$$\boldsymbol{\sigma}_0 \cdot \boldsymbol{\xi} = \nabla u_0 \cdot a_0\boldsymbol{\xi} = a_0\nabla u_0 \cdot \boldsymbol{\xi} \ \text{ for all } \boldsymbol{\xi} \in \mathbb{R}^d.$$

Note that $\boldsymbol{\xi}$ is chosen arbitrarily; we deduce that

$$\boldsymbol{\sigma}_n = a_n\nabla u_n \overset{w}{\rightharpoonup} \boldsymbol{\sigma}_0 = a_0\nabla u_0 \ \text{ in } \boldsymbol{L}^2(D) \ \text{ for a.e. } \omega \in \Omega. \tag{14}$$

Step 4. We are now ready to identify the PDEs that u_0 solves and to show that u_0 is independent of ω. By (14) and (6) we have for all $v \in H_0^1(D)$,

$$\begin{aligned}
a_0(u_0,v) - (f,v) &= a_0(u_0,v) - a_n(u_n,v_{h_n}) + (f,v_{h_n}) - (f,v) \\
&= a_0(u_0,v) - a_n(u_n,v) + a_n(u_n, v - v_{h_n}) + (f, v_{h_n} - v)
\end{aligned}$$

$$
\begin{aligned}
&= \int_D (\boldsymbol{\sigma}_0 - \boldsymbol{\sigma}_n) \cdot \nabla v \, dx + \int_D \boldsymbol{\sigma}_n \cdot (\nabla v - \nabla v_{h_n}) \, dx \\
&\quad + \int_D f(v_{h_n} - v) \, dx \\
&\leq \int_D (\boldsymbol{\sigma}_0 - \boldsymbol{\sigma}_n) \cdot \nabla v \, dx + \|\boldsymbol{\sigma}_n\|_{\boldsymbol{L}^2(D)} \|\nabla v - \nabla v_{h_n}\|_{\boldsymbol{L}^2(D)} \\
&\quad + \|f\|_{L^2(D)} \|v_{h_n} - v\|_{L^2(D)} \\
&\to 0 \quad \text{for a.e. } \omega \in \Omega.
\end{aligned}
$$

Note that u_0 is independent of ω since both a_0 and f are deterministic. Therefore, not only a particular subsequence but also the entire sequence admit convergence. ∎

Now it remains to show the convergent path (ii) in Figure 1, in which h is fixed while ε is sent to zero. Although the effective features can be described by a deterministic model with constant coefficients, the standard FEMs would generically fail to correctly pass to the limit in such a situation. An intuitive explanation is that, by Theorem 2.3, the effective coefficient is the averaged result of both the stochastic field and the interaction of ε-scale oscillations. However, the polynomial base function does not depend on the modeling parameter ε, with a fixed h, and hence could not capture any ε-scale information (e.g., see [16] for problems in periodic setting). Therefore, numerous methods including, but not limited to, MsFEMs and HMMs have been developed to find accurate approximations of the homogenized solution without resolving the ε-scale structures. Moreover, it is proved with mild assumptions in [7] that MsFEMs and HMMs can correctly pass to the limit in paths (i)–(iv) for one-dimensional problems, while the high-dimensional case remains an open problem.

However, a straightforward implementation of MsFEMs suffers from resonance between the discretization scale and the modeling parameter, i.e., the numerical error becomes large when ε and h are of the same order. Specifically, let V_h^ε denote the MsFEM space consisting of local oscillating functions; for a.e. $\omega \in \Omega$, we consider the following inequality:

$$
\|u_\varepsilon^h(\cdot,\omega) - u_\varepsilon(\cdot,\omega)\|_{L^2(D)} \leq \|u_\varepsilon^h(\cdot,\omega) - u_0\|_{L^2(D)} + \|u_0 - u_\varepsilon(\cdot,\omega)\|_{L^2(D)}, \tag{15}
$$

where $u_\varepsilon^h(\cdot,\omega) \in V_h^\varepsilon$ solves (6). When $h \approx \varepsilon$, the left-hand side could be large and might even seem to diverge for periodic homogenization problems [24]. Hence, the first term on the right-hand side of (15) does not diminish since the second term goes to zero by the standard theory of homogenization. Intuitively, by Theorem 3.2, the reason for not getting convergence is that V_h^ε may not be asymptotically dense in the solution space $H_0^1(D)$.

With the intuitive argument above, a remedy for avoiding both underresolution and resonance can be made. Indeed, the study of asymptotic compatibility enables us to construct X-MsFEMs by certain enrichments of the MsFEMs approximation space so that the diagram in Figure 1 commutes in all regimes. In particular, since the continuous piecewise linear element space is independent of ε and is dense (and thus asymptotically dense) in $H_0^1(D)$, we get the following result.

COROLLARY 3.3. *For any conforming X-MsFEMs with enrichment containing all continuous piecewise linear elements, the diagram in Figure* 1 *commutes in all regimes.*

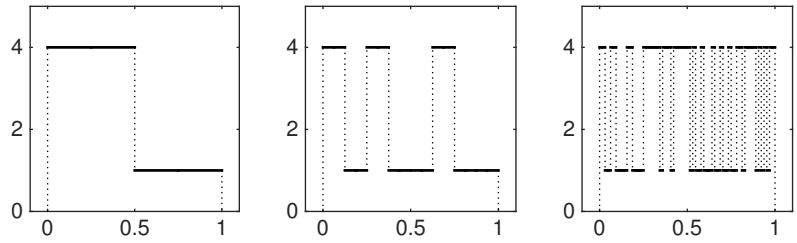

FIG. 2. *One realization of the one-dimensional tile-based random media w.r.t. tile size* $\varepsilon = 2^{-2}$, 2^{-4}, *and* 2^{-6}.

3.3. Numerical experiments. Here, numerical examples in one dimension are constructed to examine the validity of our theory. Specifically, for Theorem 3.2, we compute the error $\|u_\varepsilon^h(\cdot,\omega) - u_0\|_{L^2(D)}$ and convergence rate for $h = \varepsilon^{1/2}$, $h = \varepsilon$, and $h = \varepsilon^{3/2}$, respectively.

3.3.1. Stationary and ergodic coefficients. In comparison with Karhunen–Loève expansion that represents random fields via statistical moments, the ergodic assumptions in the homogenization theory are a more abstract notion with far less extensive practical illustration. In this section, we consider a one-dimensional tile-based random media which is known as a severe benchmark test [4]; other examples, e.g., quasi-periodic type, can be found in [25].

Specifically, let $D = [0,1]$ be uniformly divided into several disjoint intervals with length ε, each of which takes values κ_0 and κ_1 with probabilities p and $1-p$, respectively. The realization of such media w.r.t. tile size $\varepsilon = 2^{-2}$, 2^{-4}, and 2^{-6} is depicted in Figure 2, where $\kappa_1 = 1$ and $\kappa_2 = 4$ and with probability $p = 1/2$. It can be easily deduced from Theorem 3.2 that the effective coefficient is determined by

$$a_0 = \left(\mathbb{E}\left[\frac{1}{a(\omega)}\right]\right)^{-1} = \frac{8}{5}. \tag{16}$$

3.3.2. Numerical verification of asymptotic compatibility. Let $\mathcal{T}_h$ be a uniform partition of $D = [0,1]$ with mesh size h; we can take, without loss of generality, piecewise continuous linear elements $V_h = \{v_h \in C^0(\bar{D}) : v_h|_K \in \mathcal{P}_1 \text{ for all } K \in \mathcal{T}_h\}$. Now, we consider a parametric problem with the coefficients constructed in section 3.3.1: given $f = -a_0 e^x$ and $g = e^x$, find $u_\varepsilon^h(\cdot,\omega) \in \{w \in V_h : w|_{\partial D} = g\}$ such that for a.e. $\omega \in \Omega$,

$$a_\varepsilon(u_\varepsilon^h, v_h) = (f, v_h) \text{ for all } v_h \in \{w \in V_h : w|_{\partial D} = 0\}. \tag{17}$$

Then by Theorem 3.2, as h and ε tend to zero, the solution to (17) converges to the solution of the homogenized problem given below: find $u_0 \in \{w \in H^1(D) : w|_{\partial D} = g\}$ such that

$$a_0(u_0, v) = (f, v) \text{ for all } v \in H_0^1(D), \tag{18}$$

where a_0 is given in (16) and the effective solution has explicit expression $u_0(x) = e^x$.

Given the random input data as depicted in Figure 2, the numerical realizations to problem (17) in all regimes are presented in Figure 3. Note that, in the last column, all the realizations are shown to solve an elliptic problem with a constant coefficient. Namely, neither the resonance nor the underresolution does pollute the approach

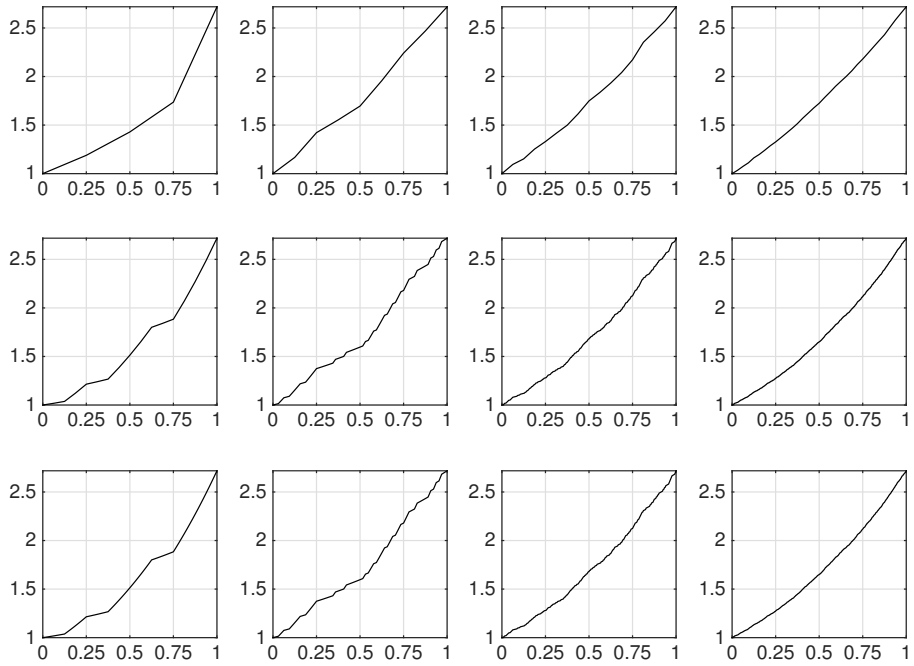

FIG. 3. *From top to bottom: numerical sample realizations* $u_\varepsilon^h(x,\omega)$ *w.r.t.* $h = \varepsilon^{1/2}$, $h = \varepsilon$, *and* $h = \varepsilon^{3/2}$. *From left to right:* $\varepsilon = 2^{-4}, 2^{-6}, 2^{-8}$, *and* 2^{-10}.

TABLE 1
Error and convergence order in L^2 *and* L_∞ *norms for different regimes using linear elements.*

ε	$\|e\|_{L^2} \times 10^{-2}$			$\|e\|_{L_\infty} \times 10^{-2}$		
	$h = \varepsilon^{1/2}$	$h = \varepsilon$	$h = \varepsilon^{3/2}$	$h = \varepsilon^{1/2}$	$h = \varepsilon$	$h = \varepsilon^{3/2}$
2^{-2}	22.63(−)	25.08(−)	25.71(−)	43.04(−)	43.58(−)	43.80(−)
2^{-4}	19.78(0.19)	12.66(0.49)	12.71(0.51)	37.62(0.19)	23.19(0.45)	23.27(0.46)
2^{-6}	8.57(1.21)	4.70(0.71)	4.70(0.72)	13.73(1.45)	11.02(0.54)	11.06(0.54)
2^{-8}	5.84(0.55)	1.70(0.73)	1.70(0.73)	9.96(0.46)	5.44(0.51)	5.45(0.51)
2^{-10}	5.59(0.06)	0.65(0.70)	0.65(0.70)	8.83(0.17)	1.54(0.91)	1.55(0.91)

to an effective solution, which validates the property of asymptotic compatibility in Theorem 3.2 for piecewise linear elements. Moreover, the numerical error $e = u_\varepsilon^h(\cdot,\omega) - u_0$ in L^2 and L_∞ norms for all scenarios are given in Table 1.

For the last two cases, i.e., $h = \varepsilon$ and $h = \varepsilon^{3/2}$, we use the partitions where all the discontinuities in the coefficient lie on grid points. Hence, the FEM with piecewise linear base functions that is used for solving the one-dimensional problem (17) can still attain second order accuracy in the infinity norm [29]. While in the case of underresolution, i.e., $h = \varepsilon^{1/2}$, only first order accuracy in the infinity norm is obtained since the ε-scale details haven't been resolved [29].

We note, however, that no convergence order is obtained from Table 1. On the one hand, it may be as in the Birkhoff's ergodic theorem where no general statement can be made about the speed of convergence [27, 28]. On the other hand, when using realizations to approach the homogenized solution, it is subject to fluctuation effects.

For the one-dimensional example, if the deviation of $1/a_\varepsilon^T(\cdot,\omega)$ from its mean $1/a_0$ is strongly mixing, the corrector theory in [7] shows that, as $\varepsilon \to 0$,

$$u_\varepsilon(\cdot,\omega) - u_0 \xrightarrow{\text{in distribution}} \varepsilon^\gamma \mathcal{N}(\cdot,\omega), \tag{19}$$

where $0 < \gamma < 1$ and $\mathcal{N}(\cdot,\omega)$ is a Gaussian random process. In other words, the error could be large even if the parameter ε is very small. Therefore, the expected value is used to deal with such a problem in the following sections.

4. Asymptotically compatible schemes for expectation. In this section, we first prove that the expected value can also converge to the same homogenized solution and its MC FE approximation inherits the property of asymptotic compatibility from numerical realizations. Moreover, specific error estimation is derived to enhance the numerical efficiency, and numerical experiments are presented to validate our statements.

4.1. Asymptotic compatibility. To begin with, we prove that the expectation $\mathbb{E}[u_\varepsilon]$ also converges to the homogenized solution u_0 as $\varepsilon \to 0$. Then, by mimicking a similar diagram in Figure 1, a discussion on the asymptotic compatibility for the MC FE approximation (2) of $\mathbb{E}[u_\varepsilon]$ is presented.

THEOREM 4.1. *The expected value of the pathwise solution to problem* (4) *satisfies*

$$\mathbb{E}[u_\varepsilon] \to u_0 \ \text{ in } L^2(D), \ \text{as } \varepsilon \to 0,$$

where u_0 *solves the homogenized problem* (5).

Proof. By the theory of stochastic homogenization, we have for a.e. $\omega \in \Omega$,

$$\|u_\varepsilon(\cdot,\omega) - u_0\|_{L^2(D)} \to 0, \ \text{as } \varepsilon \to 0.$$

On the other hand, the following standard estimate holds almost surely:

$$\|u_\varepsilon(\cdot,\omega) - u_0\|_{L^2(D)} \le \|u_\varepsilon(\cdot,\omega)\|_{L^2(D)} + \|u_0\|_{L^2(D)} \le \frac{2C}{a_-}\|f\|_{L^2(D)},$$

where C is the constant given by the Poincaré inequality.

Note that the mapping $\omega \mapsto u(\cdot,\omega)$ is measurable [12]; by Lebesgue's dominated convergence theorem, it immediately implies that

$$\mathbb{E}\left[\|u_\varepsilon(\cdot,\omega) - u_0\|^2_{L^2(D)}\right] \to 0, \ \text{as } \varepsilon \to 0.$$

Then by Jensen's inequality, we have

$$\|\mathbb{E}\left[u_\varepsilon(\cdot,\omega) - u_0\right]\|^2_{L^2(D)} \le \mathbb{E}\left[\|u_\varepsilon(\cdot,\omega) - u_0\|^2_{L^2(D)}\right] \to 0, \ \text{as } \varepsilon \to 0, \tag{20}$$

that is, $\mathbb{E}[u_\varepsilon] \to u_0$ in $L^2(D)$ as $\varepsilon \to 0$ which completes the proof. ∎

Similarly, for the numerical approximation of $\mathbb{E}[u_\varepsilon]$ via scheme (2), the question on asymptotic compatibility arises naturally: whether the diagram in Figure 4 commutes.

Note that, by Theorem 4.1 and Lemma 3.1, the paths (i) and (iv) in Figure 4 are accessible, respectively. Moreover, for arbitrary but fixed $\varepsilon \in (0,\infty)$, the conventional error estimation for the elliptic problem with stochastic coefficients [8, Theorem 4.3] implies that

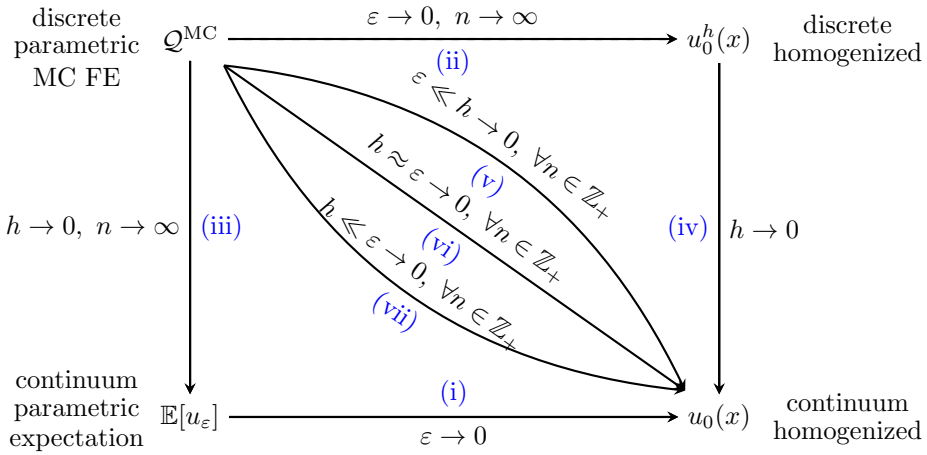

FIG. 4. *A diagram describing the convergence results of numerical homogenization.*

$$\|\mathcal{Q}^{\mathrm{MC}} - \mathbb{E}[u_\varepsilon]\|_{\mathcal{L}^2(D)} \to 0, \text{ as } h \to 0 \text{ and } n \to \infty,$$

which indicates that the convergent path (iii) holds true.

Now we consider the situation where both ε and h are sent to zero for all $n \in \mathbb{Z}_+$, i.e., the convergent paths (v)–(vii) in Figure 4, and the results are given in the following corollary.

COROLLARY 4.2. *For any conforming FEMs with approximation spaces asymptotically dense in the solution space, the expected value of the pathwise solution to* (6) *satisfies*

$$\mathbb{E}[u_\varepsilon^h] \to u_0 \text{ in } L^2(D) \text{ for any sequences } \varepsilon \to 0 \text{ and } h \to 0.$$

Furthermore, the corresponding MC FE approximation (2) *satisfies*

$$\mathcal{Q}^{\mathrm{MC}} \to u_0 \text{ in } \mathcal{L}^2(D) \text{ for any sequences } \varepsilon, h \to 0 \text{ and for all } n \in \mathbb{Z}_+.$$

Proof. For any sequences $\varepsilon \to 0$ and $h \to 0$, by Theorem 3.2, the numerical sample realization $u_\varepsilon^h(\cdot, \omega)$ converges strongly to u_0 in $L^2(D)$ almost surely. Therefore, by the arguments presented in Theorem 4.1, it immediately implies that there holds

$$\|u_\varepsilon^h - u_0\|_{\mathcal{L}^2(D)} \to 0 \quad \text{and} \quad \|\mathbb{E}[u_\varepsilon^h] - u_0\|_{L^2(D)} \to 0 \quad \text{for any sequences } \varepsilon, h \to 0. \tag{21}$$

On the other hand, the standard error bound for the MC FE estimation of $\mathbb{E}[u_\varepsilon]$ gives

$$\begin{aligned} e^{\mathrm{MC}} := \|\mathcal{Q}^{\mathrm{MC}} - u_0\|_{\mathcal{L}^2(D)} &\le \|\mathcal{Q}^{\mathrm{MC}} - \mathbb{E}[u_\varepsilon^h]\|_{\mathcal{L}^2(D)} + \|\mathbb{E}[u_\varepsilon^h] - u_0\|_{\mathcal{L}^2(D)} \\ &= \frac{1}{\sqrt{n}} \|u_\varepsilon^h - \mathbb{E}[u_\varepsilon^h]\|_{\mathcal{L}^2(D)} + \|\mathbb{E}[u_\varepsilon^h] - u_0\|_{L^2(D)} \\ &\le \frac{1}{\sqrt{n}} \|u_\varepsilon^h\|_{\mathcal{L}^2(D)} + \|\mathbb{E}[u_\varepsilon^h] - u_0\|_{L^2(D)} \\ &\le \frac{C}{a_- \sqrt{n}} \|f\|_{L^2(D)} + \|\mathbb{E}[u_\varepsilon^h] - u_0\|_{L^2(D)}, \end{aligned} \tag{22}$$

TABLE 2
Numerical error $\|\mathcal{Q}^{\mathrm{MC}} - u_0\|$ in different norms with fixed h and different ε.

Index of level (ℓ)	0	1	2	3	4
$\|\mathcal{Q}^{\mathrm{MC}} - u_0\|_{L^2}$ ($\times 10^{-2}$)	2.83	4.35	5.07	5.33	5.44
$\|\mathcal{Q}^{\mathrm{MC}} - u_0\|_{L_\infty}$ ($\times 10^{-2}$)	3.90	5.96	6.96	7.31	7.46

where C is the constant given by the Poincaré inequality [12]. By invoking (21), the right-hand side of (22) goes to zero for any sequences $(\varepsilon, h) \to (0,0)$ and $n \to \infty$.

Similarly, for fixed but arbitrary $n \in \mathbb{Z}_+$, we have

$$\begin{aligned} e^{\mathrm{MC}} &\le \frac{1}{\sqrt{n}}\|u_\varepsilon^h - \mathbb{E}[u_\varepsilon^h]\|_{\mathcal{L}^2(D)} + \|\mathbb{E}[u_\varepsilon^h] - u_0\|_{L^2(D)} \\ &\le \frac{1}{\sqrt{n}}\|u_\varepsilon^h - u_0\|_{\mathcal{L}^2(D)} + \frac{1}{\sqrt{n}}\|\mathbb{E}[u_\varepsilon^h] - u_0\|_{L^2(D)} + \|\mathbb{E}[u_\varepsilon^h] - u_0\|_{L^2(D)}, \end{aligned}$$

hence the proof is completed by invoking (21). ∎

Now it remains to examine the convergent path (ii) in Figure 4 for the standard FEMs where $h \gg \varepsilon$. Intuitively, for standard FEMs, the underresolution error could not be eliminated by using sample average since no ε-scale information is included. More precisely, by using continuous linear elements, we consider the problem (17) with a fixed mesh size $h = 2^{-9}$, a sequence of modeling parameters $\{\varepsilon_\ell = 2^{-\ell-10}\}_{\ell=0}^4$, and sample size $n = 3000$; the numerical results are presented in Table 2.

As can be seen from Table 2, even though the small-scale oscillation diminishes as $\varepsilon \to 0$, the numerical error becomes large as the ratio $r = h/\varepsilon$ grows. The reason for this is that the larger the ratio is, the worse the approximation to ε-scale structure gets. Therefore, the upscaling methods, e.g., MsFEMs and HMMs, should be used to deal with the underresolution [7]. Furthermore, X-MsFEMs may be used to overcome resonance when the discretization scale is close to the heterogeneity scale of the media as illustrated in the earlier section.

4.2. Further error analysis for the MC FE method. Although the influence of randomness can be reduced by using sample average (2), the MC simulation is known to be costly and even unaffordable. However, based on the error estimates developed for homogenization problems with deterministic limits in this section, high accuracy can be achieved by performing relatively few simulations.

Recall that the error estimation associated with approximating u_0 by $\mathcal{Q}^{\mathrm{MC}}$ takes the form

$$e^{\mathrm{MC}} \le \underbrace{n^{-\frac{1}{2}}\|u_\varepsilon^h - \mathbb{E}[u_\varepsilon^h]\|_{\mathcal{L}^2(D)}}_{\text{sampling error}} + \underbrace{\|\mathbb{E}[u_\varepsilon^h] - u_0\|_{L^2(D)}}_{\text{homogenization error}}. \tag{23}$$

Moreover, let $\mathcal{E}^{\mathrm{MC}} := \|u_\varepsilon^h - \mathbb{E}[u_\varepsilon^h]\|_{\mathcal{L}^2(D)}$, and define $\mathrm{S}_{\mathrm{err}}$ and $\mathrm{H}_{\mathrm{err}}$ as the sampling and the homogenization error, respectively. Then, by balancing errors, the MC sample size n can be determined by the following formula:

$$n^{-\frac{1}{2}}\mathcal{E}^{\mathrm{MC}} = \mathrm{S}_{\mathrm{err}} \approx \mathrm{H}_{\mathrm{err}}. \tag{24}$$

Note that by using asymptotically compatible schemes, the homogenization error diminish as $(\varepsilon, h) \to (0,0)$. Since $\mathcal{E}^{\mathrm{MC}}$ is bounded by some constant in (22), it implies

that the MC sample size n increases as $(\varepsilon, h) \to (0,0)$. However, for our problems, a key observation is that both u_ε^h and $\mathbb{E}[u_\varepsilon^h]$ can converge strongly to u_0 in $\mathcal{L}^2(D)$, that is, $\mathcal{E}^{\mathrm{MC}} \to 0$ as $(\varepsilon, h) \to (0,0)$, which enables us to perform relatively few simulations to attain high accuracy.

In fact, the MC FE approximation error also takes the form

$$\begin{aligned} e^{\mathrm{MC}} &\le \|\mathcal{Q}^{\mathrm{MC}} - \mathbb{E}[u_\varepsilon^h]\|_{\mathcal{L}^2(D)} + \|\mathbb{E}[u_\varepsilon^h] - u_0\|_{\mathcal{L}^2(D)} \\ &= \underbrace{n^{-\frac{1}{2}} \| \left(\mathbb{V}[u_\varepsilon^h]\right)^{\frac{1}{2}} \|_{L^2(D)}}_{\text{sampling error}} + \underbrace{\|\mathbb{E}[u_\varepsilon^h] - u_0\|_{L^2(D)}}_{\text{homogenization error}}, \end{aligned}$$

where the variance tends to zero as $(\varepsilon, h) \to (0,0)$ since the numerical realized values converge to the deterministic effective solutions. Moreover, one can also estimate the mean square error in a suitable norm $\|\cdot\|$ to draw a similar conclusion, i.e.,

$$\begin{aligned} \tau^{\mathrm{MC}} &:= \left\| \mathbb{E}\left[\left(\mathcal{Q}^{\mathrm{MC}} - u_0\right)^2 \right] \right\| = \left\| \mathbb{E}\left[\left(\mathcal{Q}^{\mathrm{MC}} - \mathbb{E}[u_\varepsilon^h]\right)^2 \right] + \left(\mathbb{E}[u_\varepsilon^h] - u_0\right)^2 \right\| \\ &\le \underbrace{n^{-1} \left\| \mathbb{V}[u_\varepsilon^h] \right\|}_{\text{sampling error}} + \underbrace{\left\| \left(\mathbb{E}[u_\varepsilon^h] - u_0\right)^2 \right\|}_{\text{homogenization error}}. \end{aligned} \tag{25}$$

Specifically, the variance $\mathbb{V}[u_\varepsilon^h]$ of numerical realizations, which inherits the properties of continuous problem, diminishes as both $\varepsilon \to 0$ and $h \to 0$ simultaneously and thus coincides with our statements reported before. To compensate for the lack of quantitative results based on theoretical derivations, numerical experiments are carried out in the following section to offer quantitative finding by showing the order of convergence that is not provided in our convergence theorem.

4.3. Numerical experiments. Here, we consider the following boundary value problem with stationary and ergodic coefficients: given $f \in H^{-1}(D)$ and $g \in H^{1/2}(D)$, find $u_\varepsilon^h(\cdot, \omega) \in \{w \in V_h : w|_{\partial D} = g\}$ such that for a.e. $\omega \in \Omega$,

$$a_\varepsilon(u_\varepsilon^h, v_h) = (f, v_h) \quad \text{for all } v_h \in \{w \in V_h : w|_{\partial D} = 0\}, \tag{26}$$

where the quantity of interest $\mathbb{E}[u_\varepsilon]$ is approximated by sample average (2). Without loss of generality, standard FEMs are used and specific partitions are chosen where all the discontinuities in the coefficient lie on grid points. Let $\mathcal{E}_\ell^{\mathrm{MC}} = \|u_{\varepsilon_\ell}^{h_\ell} - \mathbb{E}[u_{\varepsilon_\ell}^{h_\ell}]\|$ and $\mathcal{V}_\ell^{\mathrm{MC}} = \|\mathbb{V}[u_{\varepsilon_\ell}^{h_\ell}]\|$ for $\ell = 0, \ldots, L \in \mathbb{Z}_+$, where L^2 and L_∞ norms are used.

In such settings, numerical results are reported in this section to computationally verify the assumption

$$\mathcal{E}^{\mathrm{MC}} = \|u_\varepsilon^h - \mathbb{E}[u_\varepsilon^h]\| \le C\varepsilon^\alpha \quad \text{and} \quad \mathcal{E}^{\mathrm{MC}} = \|\mathbb{V}[u_\varepsilon^h]\| \le C\varepsilon^\beta, \tag{27}$$

where C is a generic constant, and α and β are two positive constants which change with the dimension of problem and the norm $\|\cdot\|$ of interest.

4.3.1. One-dimensional numerical experiment. We consider the model problem (26) with coefficients constructed in section 3.3.1, $f(x) = -8e^x/5$ and $g(x) = e^x$. Specifically, the sequence of modeling parameters is chosen to be $\{\varepsilon_\ell = 2^{-\ell-5}\}_{\ell=0}^{L=7}$, and the mesh sizes are given by $h_\ell = 2^{-\ell-6}$ with fixed ratio $r = 2^{-1}$ for $\ell = 0, \ldots, 7$. Furthermore, by using $n = 3000$ samples and quadratic elements, the numerical

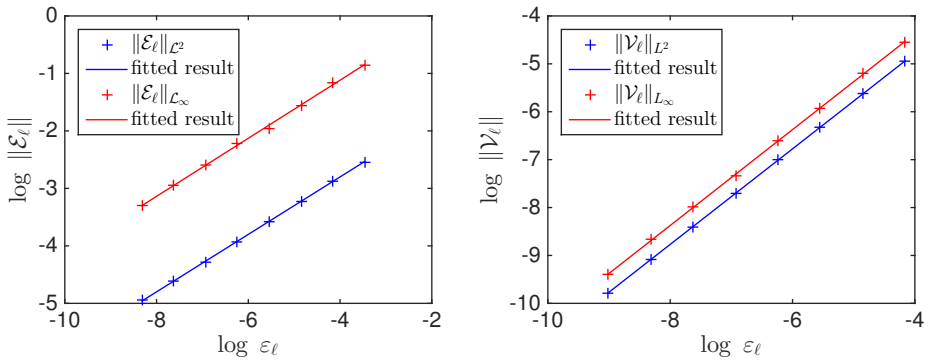

FIG. 5. *Linear fitted results of* $\mathcal{E}_\ell^{\mathrm{MC}}$ *and* $\mathcal{V}_\ell^{\mathrm{MC}}$ *for* $\ell = 0, \ldots, 7$.

TABLE 3
Linear fitted results and convergence orders of $\mathcal{E}_\ell^{\mathrm{MC}}$ *and* $\mathcal{V}_\ell^{\mathrm{MC}}$ *for* $\ell = 0, \ldots, 7$.

Index of level (ℓ)	0	1	2	3	4	5	6	7	Order
$\|\mathcal{E}_\ell^{\mathrm{MC}}\|_{\mathcal{L}^2(D)} \times 10^{-2}$	7.91	5.68	3.96	2.81	1.98	1.39	0.99	0.71	0.50
$\|\mathcal{E}_\ell^{\mathrm{MC}}\|_{\mathcal{L}_\infty(D)} \times 10^{-2}$	42.93	31.34	20.88	14.12	10.80	7.54	5.22	3.71	0.51
$\|\mathcal{V}_\ell^{\mathrm{MC}}\|_{L^2(D)} \times 10^{-4}$	70.82	36.53	17.81	9.11	4.48	2.26	1.46	0.56	1.00
$\|\mathcal{V}_\ell^{\mathrm{MC}}\|_{L_\infty(D)} \times 10^{-4}$	106.68	55.36	26.79	13.47	6.45	3.39	1.72	0.83	1.00

results concerning assumption (27) are given as follows: Figure 5 presents the linear fitted results of $\mathcal{E}_\ell^{\mathrm{MC}}$ and $\mathcal{V}_\ell^{\mathrm{MC}}$, while the computational results are given in Table 3.

As seen from Table 3, assumption (27) is substantiated with convergence orders $\alpha \approx 0.5$ and $\beta \approx 1$, which validates our statements in section 4.2. This enables us to determine the optimal sample size for different types of error and parameter value, which could greatly reduce the computational cost in contrast to the traditional MC methods.

4.3.2. Two-dimensional numerical experiment. Next, a two-dimensional model problem (26) with coefficient in a chessboard type is considered [25]. Specifically, let I_2 be the 2 by 2 identity matrix and the domain $D = [0,1]^2$ be split into squares of length $\varepsilon > 0$. We consider that the coefficient $a_\varepsilon^T(x,\omega)$ takes two values $\kappa_1 I_2$ and $\kappa_2 I_2$ on each square independently for two given positive scalars κ_1 and κ_2, with probabilities p and $1-p$, respectively.

Some realizations of such two-dimensional media with $\kappa_1 = 1$ (black), $\kappa_2 = 4$ (white), and $p = 1/2$ are depicted on the first line of Figure 6. The corresponding numerical realization with $f(x,y) = e^{xy(x-1)(y-1)}$, $g(x,y) = 0$, and a fixed ratio $r = 1$ is presented on the second line of Figure 6. Note that the right-hand side is a symmetric function centered at $(1/2, 1/2)$, and numerical realization $u_\varepsilon^h(\cdot,\omega)$ is seen to solve an elliptic problem with a constant coefficient, which matches with our theory in Theorem 3.2.

Next, $n = 5000$ samples and quadratic elements are used to numerically verify the assumption (27) with the sequence of parameter chosen to be $\{\varepsilon_\ell = 2^{-2-\ell}\}_{\ell=0}^{L=3}$, and the numerical results are given in Figure 7 and Table 4, which validate our statements.

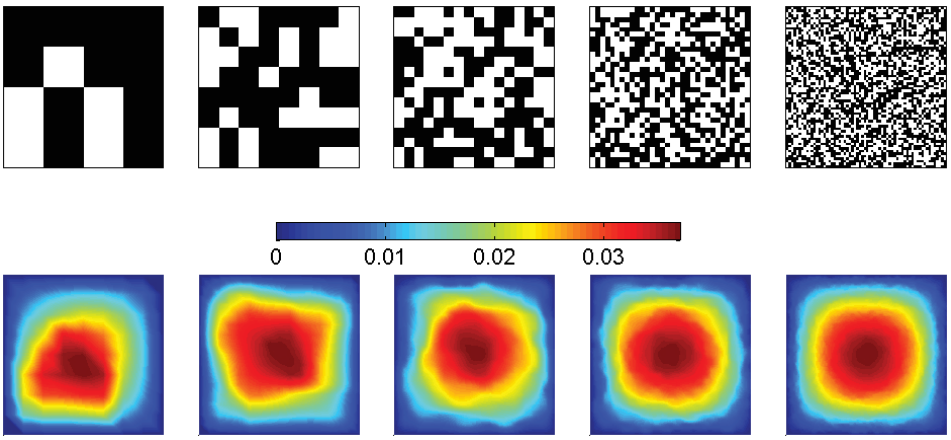

FIG. 6. *Realizations of the two-dimensional chessboard media and the corresponding solutions w.r.t.* $\{\varepsilon = 2^{-\ell}\}_{\ell=2}^{6}$.

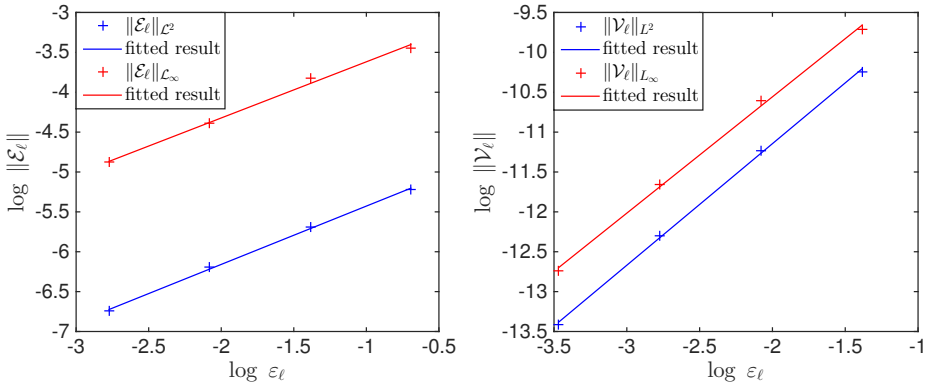

FIG. 7. *Linear fitted results of* $\mathcal{E}_\ell^{\mathrm{MC}}$ *and* $\mathcal{V}_\ell^{\mathrm{MC}}$ *for* $\ell = 0, \ldots, 3$.

TABLE 4
Linear fitted results and convergence orders of $\mathcal{E}_\ell^{\mathrm{MC}}$ *and* $\mathcal{V}_\ell^{\mathrm{MC}}$ *for* $\ell = 0, \ldots, 3$.

Index of level (ℓ)	0	1	2	3	Order
$\|\mathcal{E}_\ell^{\mathrm{MC}}\|_{\mathcal{L}^2(D)}$ $(\times 10^{-3})$	5.37	3.39	2.04	1.18	0.73
$\|\mathcal{E}_\ell^{\mathrm{MC}}\|_{\mathcal{L}_\infty(D)}$ $(\times 10^{-2})$	3.20	2.19	1.24	0.76	0.70
$\|\mathcal{V}_\ell^{\mathrm{MC}}\|_{L^2(D)}$ $(\times 10^{-5})$	3.57	1.32	0.46	0.15	1.52
$\|\mathcal{V}_\ell^{\mathrm{MC}}\|_{L_\infty(D)}$ $(\times 10^{-5})$	6.02	2.48	0.87	0.29	1.46

5. Conclusions. In this work, we first introduce the theory of asymptotic compatibility for the numerical sample realization of elliptic homogenization problems using standard FEMs, MsFEMs, and X-MsFEMs. We then demonstrate that the expected value, which also converges to the homogenized solution, provides a more attractive alternative since the convergence is less susceptible to the fluctuation effects. To evaluate the expectation, the MC FE scheme (2) is used and it is shown to inherit the asymptotic compatibility. Finally, specific error estimation is derived to further enhance the efficiency of our numerical approach.

The framework and numerical schemes developed in this paper could also be applied to high-contrast problems with additional small scale in the coefficients, stochastic optimal control problems where (4) serves as constraints, etc. Such problems await further investigations in the future [32]. In addition, we note that besides the conventional MC sampling strategy discussed in this paper, one may also invoke several techniques including, but not limit to, the quasi-MC method [11, 19], the Markov chain MC method [20], variance reduction [5, 21, 22], and reduced order basis techniques [13] to further enhance the performance of the MC scheme. It will be interesting future work to study these as well as other variants of multilevel and multiscale MC schemes arising from the asymptotic compatibility of numerical expectation presented in Corollary 4.2.

Acknowledgments. The authors would like to thank Xiaochuan Tian, Zhi Zhou, Wenjia Jing, and Guillaume Bal for numerous useful discussions. They also, would like to thank the referees for valuable suggestions.

REFERENCES

[1] A. Abdule, A. Barth, and C. Schwab, *Multilevel Monte Carlo methods for stochastic elliptic multiscale PDEs*, Multiscale Model. Simul., 11 (2013), pp. 1033–1070.
[2] A. Abdule, E Weinan, B. Engquist, and E. Vanden-Eijnden, *The heterogeneous multiscale method*, Acta Numer., 21 (2012), pp. 1–87.
[3] A. Alexanderian, *Expository paper: A primer on homogenization of elliptic PDEs with stationary and ergodic random coefficient functions*, Rocky Mountain J. Math., 45 (2015), pp. 703–735.
[4] A. Alexanderian, M. Rathinam, and R. Rostamian, *Homogenization, symmetry and periodization in diffusive random media*, Acta Math. Sci., 32 (2012), pp. 129–154.
[5] A. Anantharaman, R. Costaouec, C Le Bris, F. Legoll, and F. Thomines, *Introduction to numerical stochastic homogenization and the related computational challenges: Some recent developments*, in Multiscale Modeling and Analysis for Materials Simulation, World Scientific, River Edge, NJ, 2012, pp. 197–272.
[6] I. Babuška, R. Tempone, and G. Zouraris, *Galerkin finite element approximations of stochastic elliptic partial difference equations*, SIAM J. Numer. Anal., 42 (2004), pp. 800–825.
[7] G. Ball and W. Jing, *Corrector theory for MsFEM and HMM in random media*, Multiscale Model. Simul., 9 (2011), pp. 1549–1587.
[8] A. Barth, C. Schwab, and N. Zollinger, *Multi-level Monte Carlo finite element method for elliptic PDEs with stochastic coefficients*, Numer. Math., 119 (2011), pp. 123–161.
[9] A. Bensoussan, J. Lions, and G. Papanicolaou, *Asymptotic Analysis for Periodic Structures*, AMS, Providence, RI, 2011.
[10] A. Bourgeat and A. Piatnitski, *Approximations of effective coefficients in stochastic homogenization*, Ann. Inst. Henri Poincaré Probab. Stat., 40 (2004), pp. 153–165.
[11] R. Caflisch, *Monte Carlo and quasi-Monte Carlo methods*, Acta Numer., 7 (1998), pp. 1–49.
[12] J. Charrier, *Strong and weak error estimates for elliptic partial differential equations with random coefficients*, SIAM J. Numer. Anal., 50 (2012), pp. 216–246.
[13] E. Chung, Y. Efendiev, W. Leung, and G. Li, *Sparse generalized multiscale finite element methods and their applications*, Int. J. Multiscale Comput. Engrg., 14 (2016).
[14] C. Chu , I. Graham, and T. Hou, *A new multiscale finite element method for high-contrast elliptic interface problems*, Math. Comp., 79 (2010), pp. 1915–1955.
[15] Q. Du, Y. Tao, X. Tian, and J. Yang, *Robust a posteriori stress analysis for quadrature collocation approximations of nonlocal models via nonlocal gradients*, Comput. Methods Appl. Mech. Engrg., 310 (2016), pp. 605–627.
[16] Y. Efendiev, *The Multiscale Finite Element Method (MsFEM) and Its Applications*, Ph.D. thesis, Applied and Computational Mathematics, Caltech, Pasadena, CA, 1999.
[17] Y. Efendiev, C. Kronsbein, and F. Legoll, *Multilevel Monte Carlo approaches for numerical homogenization*, Multiscale Model. Simul., 13 (2015), pp. 1107–1135.
[18] L.C. Evans, *Partial Difference Equations*, AMS, Providence, RI, 2010.
[19] M. Giles, *Multilevel Monte Carlo methods*, Acta Numer., 24 (2015), pp. 259–328.

[20] W. Gilks, S. Richardson, and D. Spiegelhalter, *Markov Chain Monte Carlo in Practice*, CRC Press, Boca Raton, FL, 1995.
[21] A. Gloria and F. Otto, *An optimal variance estimate in stochastic homogenization of discrete elliptic equations*, Ann. Probab., 39 (2011), pp. 779–856.
[22] A. Gloria, S. Neukamm, and F. Otto, *An optimal quantitative two-scale expansion in stochastic homogenization of discrete elliptic equations*, ESAIM Math. Model. Numer. Anal., 48 (2014), pp. 325–346.
[23] M. Gunzburger, C. Webster, and G. Zhang, *Stochastic finite element methods for partial differential equations with random input data*, Acta Numer., 23 (2014), pp. 521–650.
[24] T. Hou, X. Wu, and Z. Cai, *Convergence of a multiscale finite element method for elliptic problems with rapidly oscillating coefficients*, Math. Comp., 68 (1999), pp. 913–943.
[25] V. Jikov, S. Kozlov, and O. Olenik, *Homogenization of Differential Operators and Integral Functionals*, Springer, New York, 2012.
[26] S. Kozlov, *Averaging of random operators*, Mat. Sb., 151 (1979), pp. 188–202.
[27] S. Kakutani and K. Petersen, *The speed of convergence in the Ergodic Theorem*, Monat. Math., 91 (1981), pp. 11–18.
[28] U. Krengel, *On the speed of convergence in the ergodic theorem*, Monat. Math. 86 (1978), pp. 3–6.
[29] Z. Li, *The immersed interface method using a finite element formulation*, Appl. Numer. Math., 27 (1998), pp. 253–267.
[30] G. Papanicolaou and S. Varadhan, *Boundary value problems with rapidly oscillating random coefficients*, Random Fields, 1 (1979), pp. 835–873.
[31] R. Smith, *Uncertainty Quantification: Theory, Implementation, and Applications*, Comput. Sci. Eng. 12, SIAM, Philadelphia, 2013.
[32] Q. Sun and Q. Du, *Numerical stochastic homogenization of a distributed optimal control problem*, submitted.
[33] L. Tartar, *The General Theory of Homogenization: A Personalized Introduction*, Lect. Notes Unione Mat. Ital. 7, Springer, New York, 2009.
[34] X. Tian and Q. Du, *Asymptotically compatible schemes and applications to robust discretization of nonlocal models*, SIAM J. Numer. Anal., 52 (2014), pp. 1641–1665.